9 (2021) 100083

Contents lists available at ScienceDirect

Biosensors and Bioelectronics: X

journal homepage: www.journals.elsevier.com/biosensors-and-bioelectronics-x

Gas sensor array to classify the chicken meat with *E. coli* contaminant by using random forest and support vector machine

Suryani Dyah Astuti [a,*], Mohammad H. Tamimi [a], Anak A.S. Pradhana [b], Kartika A. Alamsyah [b], Hery Purnobasuki [c], Miratul Khasanah [d], Yunus Susilo [e], Kuwat Triyana [f], Muhammad Kashif [b], Ardiyansyah Syahrom [g]

[a] Department of Physics, Faculty of Science and Technology, Universitas Airlangga, Surabaya, 60115, Indonesia
[b] Biomedical Engineering Magister Program, Faculty of Science and Technology, Universitas Airlangga, Surabaya, 60115, Indonesia
[c] Department of Biology, Faculty of Science and Technology, Universitas Airlangga, Surabaya, 60115, Indonesia
[d] Department of Chemistry, Faculty of Science and Technology, Universitas Airlangga, Surabaya, 60115, Indonesia
[e] Faculty of Engineering-Universitas Dr Soetomo, Surabaya, Indonesia, 60118, Indonesia
[f] Department of Physics, Faculty of Matematic and Natural Science, Universitas Gadjah Mada Yogyakarta, Indonesia
[g] Department of Applied Mechanics and Design, Faculty of Mechanical Engineering, Universiti Teknologi Malaysia, 81310, Johor Bahru, Malaysia

ARTICLE INFO

Keywords:
Food security
Chicken meat
E. coli
Support vector machine
Random forest
Gas sensor array

ABSTRACT

Microbes such as *Escherichia coli* (*E. coli*) can easily contaminate raw chicken meat in clean conditions, causing decay and unpleasant scents. This study aims to characterize gas patterns by comparing fresh chicken meat and *E. coli* bacteria contaminated chicken meat based on shelf life using a Gas Sensor Array (GSA) system (MQ2, MQ3, MQ7, MQ8, MQ135, and MQ136) on electronic nose. The findings revealed GSA capability to detect a variety of typical gas patterns formed by the samples. This gas detection property is indicated by the appearance of the variance in the sensors output voltage pattern for each sample variation. The data for fresh and contaminated samples were classified by the random forest (RF) classifier with 99.25% and 98.42% precision, respectively. Furthermore, the support vector machine (SVM) classifier correctly identified the fresh and contaminated samples with 98.61% and 86.66% accuracy, respectively. This finding offers insight for GSA capability in classifying chicken meat contaminated with *E. coli* using an RF and SVM.

1. Introduction

The consumption of chicken meat, especially broiler is increasing every year. However, this increasing consumption rate is not followed by improvement in the quality control system of chicken meat production. In traditional markets chicken meat is sold uncovered, exposed to ambient air at room temperature and not thoroughly cleaned or washed, so it is easily contaminated with bacteria (Hygreeva and Pandey, 2016). The pH value in sliced chicken muscles is about 7.0 and it decreases during anaerobic glycolysis (postmortem glycolysis) process. After rigor mortis, the chicken meat pH value becomes 5.5–6.4 and the final optimum pH value in acceptable chicken meat fall between 5.5-5.9. Meat that contains water, is rich in nitrogen and having acidic pH can be a suitable growth medium for microorganisms such as bacteria (Hygreeva and Pandey, 2016). The maximum limit of microorganism contamination in chicken meat is 1×10^6 CFU/g.

Chicken meat (poultry) is highly potential to be infected by *Escherichia coli* (*E. coli*) (O157: H7), which is a pathogenic microorganism causing hemorrhagic enteritis in human (Astuti et al., 2019a,b). This contaminated meat can lead to several diseases such as diarrhea, dysentery, kidney and bladder infections, as well as pneumonia and meningitis (Oliver, 2019; Pradhana et al., 2020). Meat contamination can happen through the transfer of fecal pathogens originating from feces or digestive tract into muscle tissue during cutting process. Meat damage or decay is characterized by the presence of fishy, rancid or other unpleasant odors and so called off odor (Bueno et al., 2013). This decay is also followed by the formation of sticky mucus on the meat surface from the production of dextran, exopolysaccharides or the growing microbe cells. The color change in chicken meat is caused by hydrogen sulfide (H_2S) production during poultry meat microbes decay (Smolander et al., 2002). In other studies, it is stated that the color changes in decayed chicken meat were occurred due to the presence of CO and N (Salinas

* Corresponding author.
E-mail addresses: suryanidyah@fst.unair.ac.id, suryanidyah@fst.unair.ac.id (S.D. Astuti).

https://doi.org/10.1016/j.biosx.2021.100083
Received 10 June 2021; Received in revised form 10 September 2021; Accepted 15 September 2021
Available online 30 September 2021

et al., 2012).

The frequently used conventional method for meat damage and spoilage testing is the Eber test. This test gives a qualitative result in the form of gas output on the tube wall, where the amino acid chain will be broken by strong HCl acid so that NH_4Cl (gas) will be formed. It is also known that fresh, cold, and frozen meat will not produce NH_4Cl after being tested using Eber solution since there is no NH_3 gas production (Premarathne et al., 2017). Meanwhile, decayed meat will emit white gas (NH_4Cl) because it produces NH_3 which indicates the presence of *E. coli* bacteria. The Eber test is less practical since it requires additional HCl to break down amino acids and it is not real-time. To overcome this problem, practical instruments and methods should be used to generate faster data analysis, then it leads the researchers to develop an Electronic nose (e-nose) system.

E-nose olfactory system has been developed and used in various fields. This system is useful, among others, in testing the quality of food products, namely (i) monitoring process, (ii) determining shelf life, (iii) evaluating damage, (iv) evaluating toxicity and (v) quality control studies (Peris and Escuder-Gilabert, 2009). The disadvantage of E-nose is its inability to display information about the compounds in the sample as offered by the GC/MS analysis technique. This system is based on a comprehensive approach called 'electronic volatile fingerprinting' (O'Sullivan et al., 2003).

In the food industry, e-nose can be used as odor identification to monitor production processes, such as detecting pathogenic fungi that attack strawberry crops (Pan et al., 2014). Arshak's research in 2004 proved that e-nose is able to sense the existence of microorganism pollution in food products, by sensing the odor patterns result coming from the organism's metabolic processes (Arshak et al., 2004). In 2015, Triyana succeeded in making a gas sensor that detects the aroma of tempeh during fermentation to verify the tempeh aroma profile related to microorganisms growth (Triyana et al., 2015). Based on its advantages, which are rapid and non-destructive detection, the e-nose has been widely used in many types of meat evaluation (Wijaya et al., 2017). Whereas in medical field, e-nose is also able to detect bacterial biofilms that cause many oral diseases, such as *Streptococcus mutans* (Astuti et al., 2019a,b).

In recent years, the development of electronic sensor technology such as electronic tongue and e-nose has shown favorable application for pattern detection in daily life (Wojnowski et al., 2017). This study aims to characterize the fresh chicken meat and *E. coli* bacteria contaminated chicken meat based on the shelf time by using gas sensor array (GSA) system on the e-nose.

2. Material and methods

2.1. E. coli specimen

Specimens of *E. coli* were acquired from Central Health Laboratory Surabaya, Indonesia. Bacteria cultures on Trypticase Soy Agar medium (Merck) were added to 10 mL of Trypticase Soy Broth (Merck) medium and shaken to give an optical density of 0.5 McFarland (10^{-13} CFU/mL). Then the liquid culture was stored at 37 °C temperature for 24 h. Afterward, bacterial density was measured using an ELISA reader ($\lambda = 480$ nm).

2.2. Chicken meat preparation

One Kg of broiler chicken meat obtained from the local market was diced into 2 × 2 cm size then classified as 2 groups. The first group, which contained 300 g of meat, was placed in a glass beaker and was not given any treatments. The second group, containing equal weight of meat, was intentionally contaminated with *E. coli* bacteria. The samples were tightly closed to avoid contamination from other bacteria, then stored in an incubator at 37 °C for 24 h. Gas produced in chicken meat was then to be observed by using e-nose at 4 h interval.

2.3. Gas sensor

In this study, e-nose system containing 6 sensors, i.e MQ2, MQ3, MQ7, MQ8, MQ135, and MQ136. The e-nose instrumentation system uses Arduino Uno Atmega 328B and data collection system linked to a computer device using LabVIEW software. Each sensor is capable of detecting a certain type of gas (Astuti et al., 2019a,b). MQ2 can detect LPG and propane 200–5000 ppm, butane: 300–5000 ppm methane: 5000–20000 ppm, H_2: 300–5000 ppm and Alcohol:100–2000 ppm. MQ3 can detect alcohol, benzene, CH_4, hexane, LPG, CO and air with detection range 0.1–10 ppm. MQ7 can detect CO, H_2, LPG, CH_4, Alcohol, air with detection range 20–2000 ppm. MQ8 can detect H_2, LPG, CH_4, CO, Alcohol, air with detection range 60–1500 ppm. MQ135 can detect NH_3, air, alcohol, NH_4, toluene, acetone with detection range 10–300 ppm and benzene:10–1000 ppm. MQ136 can detect air, CO, NH_4 and H_2S with detection range 10–300 ppm. Fig. 1 shows the e-nose experimental set up for this study.

The principle diagram of e-nose showed in Fig. 1. Before the series of sensing processes, e-nose preheating is carried out for 30 min. The series of sensing processes take place in 3 stages, namely baseline, sensing, and purging. In the baseline process, pipe 3 will inhale the target clean air as a control and flow into the inlet hose to the chamber with the valve closing pipes 1 and 2 so that the clean air is not mixed with the odor from sample. The baseline process lasts for 60 s because in that time span all sensors are in a steady state. In the sensing process, the valve closes pipe 3 and opens pipe 1 leading target odor to flow into the chamber. Slowly the odor of the sample fills the chamber and is responded by the sensor to produce a certain voltage output. The sensing process lasts for 100 s. In the purging process, the valve closes hoses 1 and 3, opening hose 2 allowing the odor of the sample that has been sensed to flow back into the sample tube. The purging process which lasts for 120 s aims to clean the gas contained in the chamber. When the target gas is contained in the chamber, the sensing mechanism by the gas sensor takes place so that each gas sensor can produce an output as voltage values. The flow rate of gas is 0.9 L/m.

2.4. Treatments

The detection of chicken meat quality performed based on the concentration of gas produced by chicken meat at various storage times. The samples were divided into 7 groups. Group K is a control group of chicken meat without *E. coli* bacterial contaminants by measuring the response of the gas sensor array at time variations of 4; 8; 12; 16; 20; and 24 h. Group T is a control group of chicken meat with *E. coli* bacterial contaminants by measuring the response of the gas sensor array at time variations of 4; 8; 12; 16; 20; and 24 h. The sampling frequency of sensors are 180 with sensing time 280 s. The flow rate of gas is 0.9 L/m. Afterward, the data from sensor detection were classified by the random forest (RF) and support vector machines (SVM) classifiers and then continue to results analysis.

2.5. Computational analysis

2.5.1. Feature extraction

Feature extraction is a compulsory part before sensor-based data classification. There are many techniques available for feature extraction i.e principal component analysis (PCA), textural and statistical features. In (Tozlu et al., 2021), the researchers investigated whether or not different diseases (e.g., stable coronary artery disease, myocardial infarction) can be diagnosed using human breath on an electronic nose by utilizing statistical features such as mean, skewness, kurtosis, and derivate variance. They were able to classify the disease with 97.9% accuracy. In the current study design, we utilized six statistical features: mean, kurtosis, median, standard derivation, skewness, and variance. These features were extracted using MATLAB. The list of statistical features:

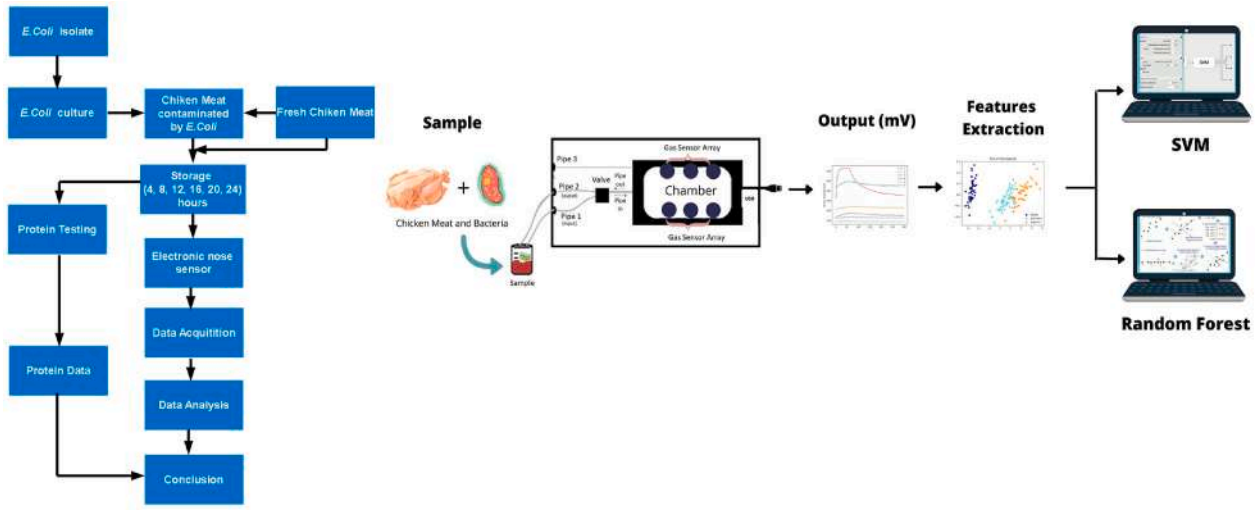

Fig. 1. Diagram of procedure and experimental set-up.

$$Mean(\overline{K}) = \frac{1}{N}\sum_{I=1}^{N} K_I \tag{1}$$

$$\text{kurtosis(K)} = \frac{\sum_i^N (K_i - \overline{K})^4}{N\sigma^4} \tag{2}$$

$$Median = median(K) \tag{3}$$

$$Skewness(K) = \frac{\sum_i^N (K_i - \overline{K})^3}{N\sigma^3} \tag{4}$$

$$variance(K) = \frac{1}{N}\sum_{i=1}^{N} (K_i - \overline{K})^2 \tag{5}$$

$$\text{Standard Deviation(K)} = \sqrt{\frac{1}{N}\sum_{i=1}^{N} (K_k - \overline{K})^2} \tag{6}$$

In feature extraction process, the original data were normalized using min-max scaler to map the values between (0,1). The formula of min-max scaler is given below:

$$x_{scaled} = \frac{x - x_{min}}{x_{max} - x_{min}} \tag{7}$$

After scaling the dataset, the feature extraction process was applied. All features were extracted using windowing method, in this method one record was considered as a one window. Each window gave six statistical features which are mentioned above. The sample of collected features is shown in Table 1. After feature extraction, the featured values were fed into machine learning models for classification.

2.5.2. Artificial neural network (ANN)

An ANN is the mathematical function of animal brains. Neuron in animal brain uses the dendrites to retrieve signal while an ANN defines the importance of inputted signal and then makes the decision whether to send the signal to the next neuron. When we feed a signal to the ANN network it retrieved by dendrites (input variable x), each input signal will be multiplied by weighted (w), the value of weight (w) assigned according to the importance of the signal and generate an output signal (y). The input data are calculated by the neuron cell body, and the signal passed the cell body according to its activation function. When we pass input to the dendrite, the activation function may be represented using the below formula:

$$y(x) = f\left(\sum_{k=1}^{N} w_k x_k\right)$$

In the above formula, the N represents the input signal (dendrites), and w is referring to the weight, that multiplies with inputs (represented by x_k). The summation of this formula is feed into the activation function f (x), and the y (x) is the output from the activation function. The strength of ANN can be determined as model of a complex pattern of the input signal by making input data correlations. Despite having some weakness, they can create overfitting, that will reduce the accuracy (Chang et al., 2018; Chen et al., 2020). We used the Weka tool to build a classification model.

2.5.3. Support Vector Machines (SVM)

SVM classifier is popular due to hyperplane creation, also called a flat boundary, this hyperplane creates homogenous partitions by dividing the space. By doing this, SVM is powerful enough to build a complicated relationship. Through kernel trick, the SVM classifier can separate the

Table 1
Sample features data for chicken meat mixed with *E. coli*

No.	Mean	Median	Standard deviation	Skewness	Kurtosis	Variance	Label
1	3.013	3.274	0.539	−0.658	1.616	0.291	unhealthy
2	3.043	3.279	0.564	−0.518	1.467	0.318	unhealthy
3	3.065	3.279	0.542	−0.573	1.584	0.294	unhealthy
4	3.088	3.305	0.489	−0.589	1.543	0.240	unhealthy
5	3.013	3.275	0.539	−0.658	1.616	0.291	unhealthy
6	2.374	2.617	0.653	−0.639	1.853	0.427	healthy
7	2.387	2.604	0.621	−0.568	1.833	0.386	healthy
8	2.226	2.447	0.448	−0.689	1.723	0.201	healthy
9	2.247	2.418	0.468	−0.576	1.738	0.219	healthy
10	2.183	2.370	0.425	−0.598	1.722	0.180	healthy

data among higher features space. The SVM kernel can be represented by the following formula:

$$K\left(\overrightarrow{x_i},\ \overrightarrow{x_j}\right)\ =\ \varphi(\overrightarrow{x_i})\ \times\ \left(\overrightarrow{x_j}\right)$$

In the above equation ϕ(x) is referring to a function that can shift the features vector x_i and x_j, then merge both features into a single feature. To classify different domains of data, many kernel functions of SVM have been developed. Linear SVM classifier does not affect the transformation of data. The polynomial SVM kernel using degree d, transform the data by adding simple non-linear. A radial base kernel is another type of SVM kernel that is quite similar to ANN, it can classify different types of data efficiently (Lantz et al., 2013; Chen et al., 2020)).

In current study we aim to classify fresh and contaminated chicken meat. So, SVM is categorized into supervised learning algorithm in machine learning, that analyse the given dataset and find out the patterns in data: this supervised algorithm can perform classification as well as regression analysis (Wei and Wang, 2014; Brudzewski et al., 2004). Based on statistical learning theory, Cortes and Vapnik proposed SVM as an efficient and highly-precised classification approach (Cortes and Vapnik, 1995). Here are some mathematical steps of SVM algorithm implementation.

1. SVM algorithm usually determine the regression model function by using following minimization function.

$$min\frac{1}{2}w^2 + c\ \sum_{i=1}^{m}\left(\xi_i^* + \xi_i\right)$$

$$s.t.\left\{\begin{array}{l} y_i - w.\xi(x)\ -\ b\ \le \varepsilon\ +\ \xi_i^* \\ w.\xi(x))\ +\ b\ -\ y_i \le \varepsilon\ +\ \xi_i \\ \xi_i^*.\ \xi\ \ge 0\ \left(i =\ 1, 2\ , 3, 4, \ldots m\right) \end{array}\right)$$

In above equation the w shows weight of the vector, likewise $\frac{1}{2}w^2$ is showing complexity of the model, penalty factor is indicated with c, ξ_i^* and ξ_i are indicating the relaxation component, $\xi(x)$ shows the non-linear transformation function, b is indicating the offset and ε is the upper limit of error.

2. The Lagrange multiplier are created now, which can be represented by α_i^* and α_i. The following equations are showing the optimization model.

$$max - \frac{1}{2}\ \sum_{i,j=1}^{m}\left(\alpha_i^* -\ \alpha_i\right)\ \left(\alpha_i^* -\ \alpha_i\right)k(X_i,\ X)\ +\ \sum_{i=1}^{m}\alpha_i^*(y_i -\ \varepsilon) -\ \sum_{i=1}^{m}\alpha_i(y_i -\ \varepsilon)$$

$$s.t\left\{\begin{array}{l} \sum_{i\ =\ 1}^{m}\alpha_i\ =\ \sum_{i\ =\ 1}^{m}\alpha_i^* \\ 0 \le\ \alpha_i,\ \alpha_i^*\ \le\ c(\ i =\ 1, 2, 3, 4, ..m) \end{array}\right.$$

3. Whereas the SVM function for regression problem can be obtain by solving above equations.

$$f(x)\ =\ \sum_{i=1}^{m}\left(\alpha_i - \alpha_i^*\ \right)k(X_i,\ X)\ + b$$

$$k\left(X_i, X_j\right)\ =\ \exp\left(\ -\frac{X_i -\ X_j^{\ 2}}{2\sigma^2}\right)\ =\ \exp\left(\ -\gamma X_i -\ X_j^{\ 2}\right),\ \gamma > 0$$

In SVM calculation, two parameters are important to adjust. The first parameter is penalty factor which is indicated by c and the second parameter is kernel which is indicated by γ.

2.5.4. Random forest (RF)

Kam proposed the RF algorithm for the first time in 1995. The RF is frequently employed in wide range of practical applications (Nitze et al., 2015; Abdel-Rahman et al., 2014). The decision tree can be created quickly, training hundreds of them is faster than training an ANN (Men et al., 2018). An RF classifier is a combination of random-trees, different decision trees arranged in such a way to get the diversity among trees (Cortes and Vapnik, 1995). RF classifier can easily classify high dimensionality features data (Chen et al., 2020). An RF classifier can reduce generalization error by increasing the number of trees in it. Correlation between individual trees and their strength can boost up the accuracy of the random forest (Breiman, 2001). The computational steps of RF algorithm are: The resampling can be obtained be using Bootstrap for generating T training sets TS1, TS2, and so on, then corresponding decision trees will be calculated for every training set C1, C2, C3 and so on. Pruning is not done because each tree is fully developed. In order to acquire the matching class for test set sample X, a test is run utilizing each decision tree C1(X), C2(X),…, CT(X). Last the test set sample X is chosen by voting as the individual in T decision trees with the greatest outputs, and the prediction is then completed.

3. Result and discussion

The MQ sensor is a metal oxide semiconductor (MOS) type gas sensor or so called chemiresistors because its tracking uses a shift in the resistance of the sensing material. The sensor tracking system uses a simple voltage partition network, so gas content can be tracked. The value of the output milli voltage (mV) detected by the sensor is proportional to the gas concentration. If the gas content is high, the output voltage will also be high and vice versa. Then the MQ gas sensor analog signal is connected to the LM393 high precision comparator, for signal digitization. That is why the reading of the sensor response results by the computer is in the unit of a voltage in mV. This voltage is generated from the change in the sensor resistance value which is directly calculated to be the voltage by the minimum circuit of the MQ sensor system.

3.1. Gas sensor array (GSA) responses to samples

Each GSA on the e-nose generates output voltage as distinctive patterns according to the sample characteristics. The specific pattern produced by each sensor can be observed from the change in the resulting voltage value. The outcome of the GSA responses on the fresh chicken meat sample group without *E. coli* bacterial contaminants and with *E. coli* bacterial contaminants are shown in Fig. 2. Fig. 3 shows E-nose patterns in various sample groups.

E-nose is a system that detects and recognizes the object based on its odor. The signal response generated by e-nose is able to manifest in the correlation between the concentration and the odor produced by chicken meat. The higher the voltage produced by e-nose, the higher the concentration of gas produced by chicken meat. Whereas, the fluctuation of the voltage signal indicates odor that has a distinctive pattern for every variation in chicken meat. Fig. 2 show an increase in sensor response as higher voltage fluctuations in chicken meat samples contaminated with *E.coli* bacteria. Voltage fluctuation indicates that bacterial contaminants can produce a specific fluctuation pattern traceable by the sensor. The resulting stress response is adequate and shows a stable tendency during the sensing process.

The sensor response pattern of each sample measured using e-nose shows a typical output pattern that varies depending on the type and the variation in shelf life (Fig. 3). It also shows the odor pattern of chicken meat complexity, with chicken meat contaminated with *E. coli* is more complex than the odor output pattern of *E. coli* bacteria. After the extraction process is complete, the data are refined with different classifiers.

3.2. Results of classification

Present study design demonstrated two conditions, the first was for

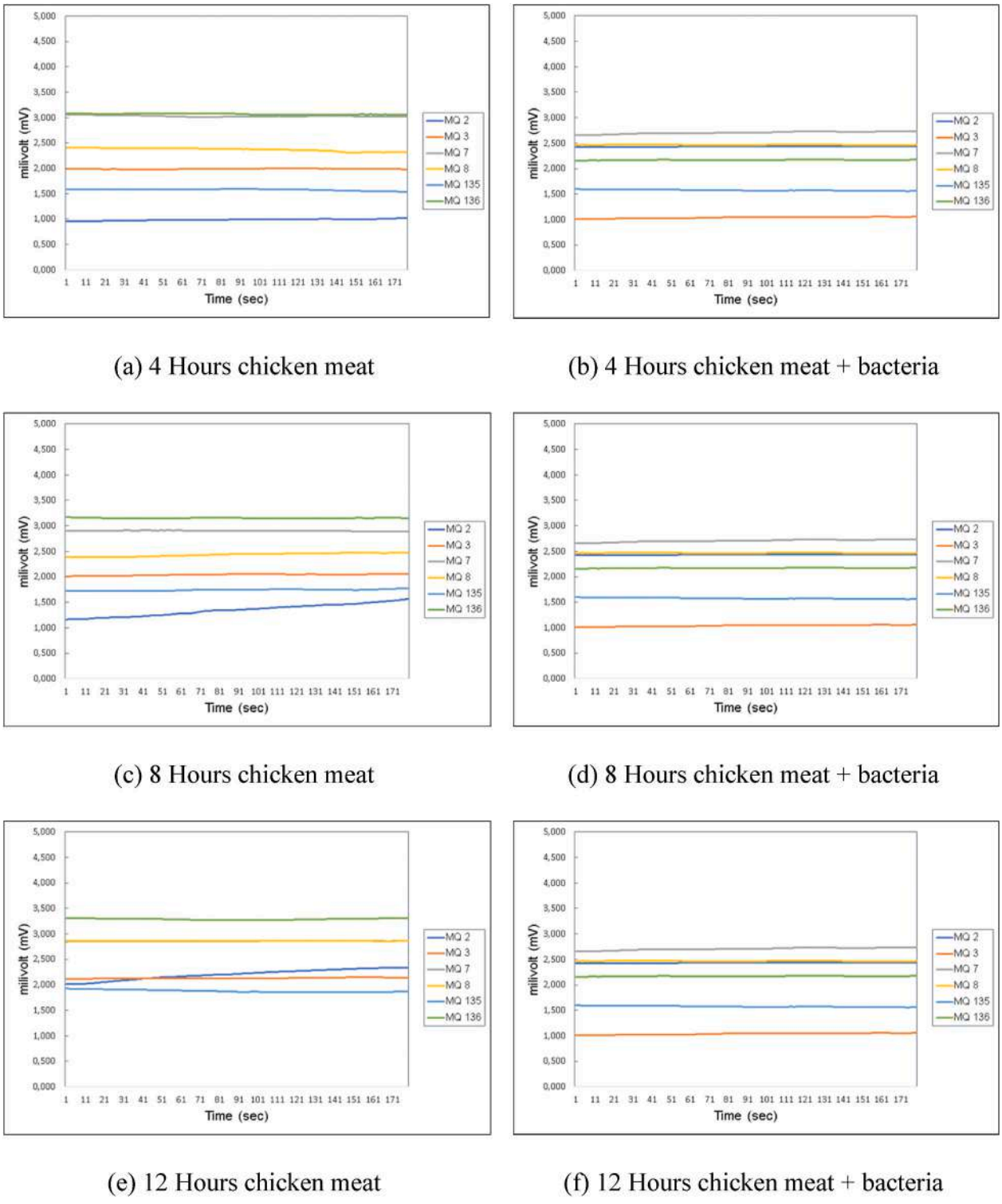

Fig. 2. Graph of GSA responses for fresh chicken meat samples with and without *E. coli* contaminants at shelf life of (a & b) 4 h; (c & d) 8 h; (e & f) 12 h; (g & h) 16 h; (i & j) 20 h; (k & l) 24 h.

observation and classification of chicken meat, the second was based on chicken meat mixed with *E. coli*. Both conditions were further divided into two sub-conditions based on healthy and unhealthy meat of chicken. The data were labeled for supervised machine learning analysis in the classification of healthy and unhealthy chicken meat. Data labeling followed by extraction of statistical features using Matlab (section 1.1). Statistical features of sample data are shown in Table 1.

After retrieving statistical features, the data were classified by Weka tool through two classifiers: SVM and RF. Initially the classification of chicken meat was performed, which showed a high level of accuracy for chicken meat while similarly the classification on RF and SVM classifier portray accuracies of 99.25% and 98.61% respectively. The accuracies of both classifiers are shown in Table 2.

Moreover, an experimentally amalgamized chicken meat with *E. coli*

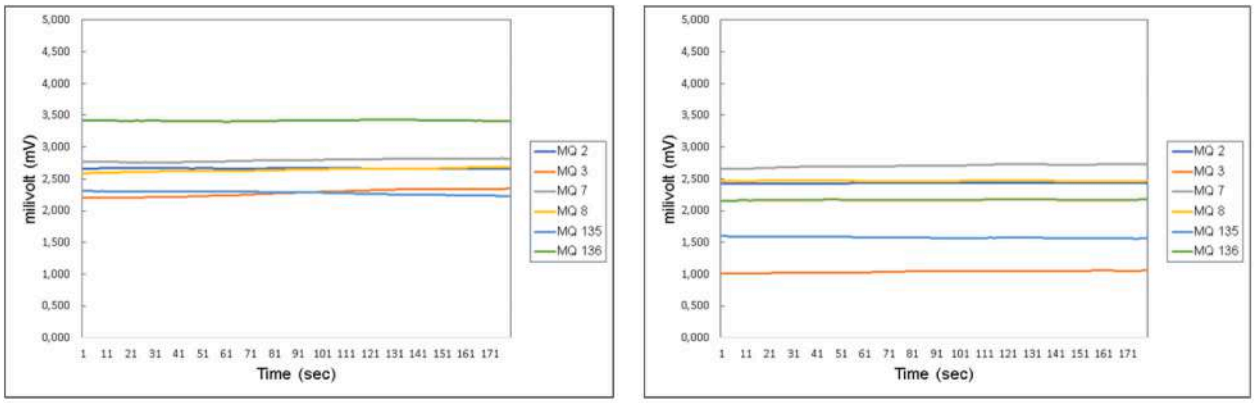

(g) 16 Hours chicken meat. (h) 16 Hours chicken meat + bacteria.

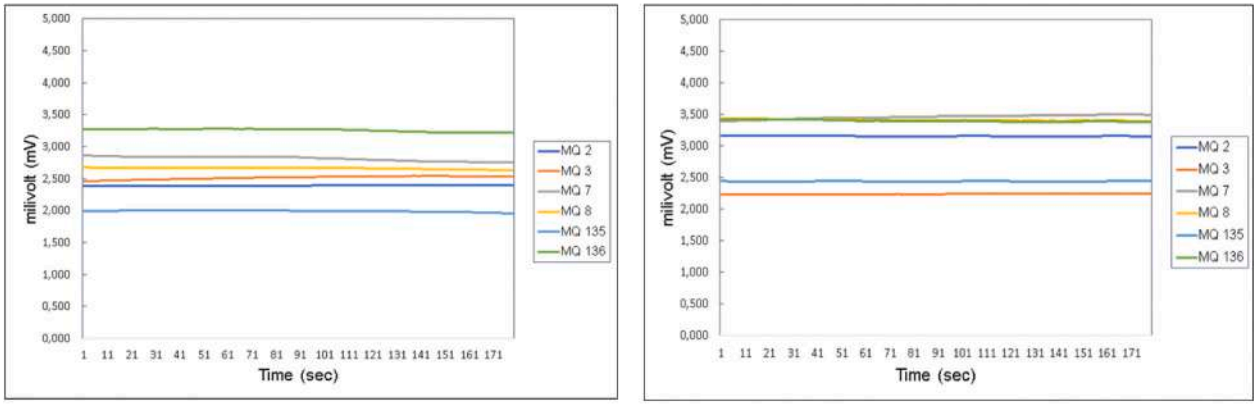

(i) 20 Hours chicken meat (j) 20 Hours chicken meat + bacteria

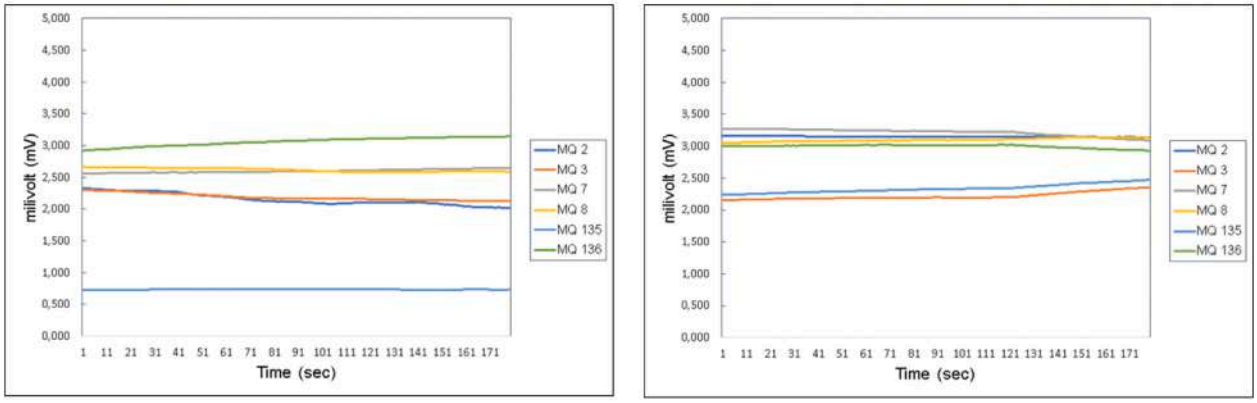

(k) 24 Hours chicken meat (l) 24 Hours chicken meat + bacteria

Fig. 2. (*continued*).

was classified through above mentioned classifiers. For this a high level of accuracy achieved on RF 98.42% while SVM classifier showed 86.66%.

The RF classifier had higher accuracies for fresh chicken meat and contaminated meat, respectively, of 99.25% and 98.42% accuracy. These values are more precise and accurate than those recorded by Mirzaee-Ghaleh et al. (2020) in fresh and thawed chicken meat with accuracies of 95.2% and 94.67%, respectively, using the fuzzy K-nearest neighbors (F–KNN) algorithm (Mirzaee-Ghaleh et al., 2020). The novelty of current study is in terms of the use of RF classifier produced higher accuracy than F–KNN algorithm, through e−nose which act as guideline for future researchers.

The current research was also more accurate than related studies that used PCA to detect food quality using a fuzzy wavelet network, and image processing and artificial intelligence to estimate the freshness of chicken meat, with accuracies of 95.71% and 80.2%, respectively (Kodogiannis, 2017; Fatahi et al., 2017).

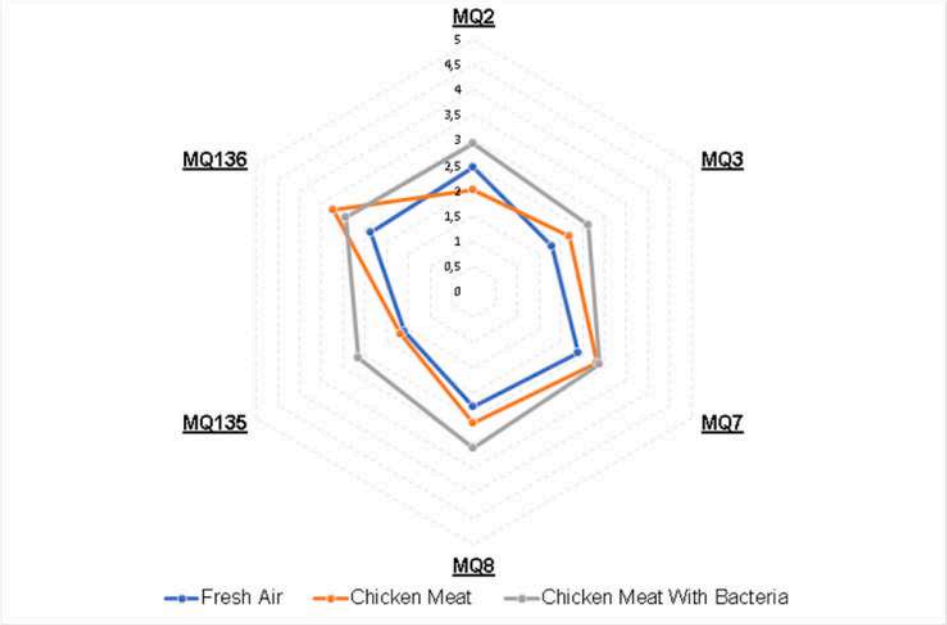

Fig. 3. E-nose patterns in various sample groups.

Table 2
Detailed accuracy of both classifiers on chicken meat only and chicken meat mixed with *E. coli*

Meat	Classifier	TP Rate	FP Rate	Precision	Recall	F-Measure	MCC	ROC Area	PRC-Are
Chicken meat only	RF	0.993	0.028	0.993	0.993	0.993	0.973	1.000	1.000
	SVM	0.986	0.016	0.987	0.986	0.986	0.951	0.985	0.983
Chicken meat mixed with *E. coli*	RF	0.984	0.023	0.984	0.984	0.984	0.965	0.999	0.999

3.3. The damage indicator

Protein content variation in meat influence the nutritional quality and the composition of meat. The meat consists of water, protein, fat, carbohydrates and ash (Ferioli and Caboni, 2010). Ammonia gas is type of odor generated from spoiling chicken meat, as an indicator of protein damages on it (Yashoda et al., 2001). This gas is generally produced by bacteria (Lázaro et al., 2015). Total volatile base (TVB) is one of the parameters for checking the freshness of fishery products in a laboratory. Total volatile base of nitrogen (TVB-N) consisting mainly of trimethylamine (TMA) and ammonia, is used as a quality criterion for feed ingredients. TVB-N is an appropriate criterion for determining product quality, including proteins component, because most TVNs containing NPN are also utilized as indicators to verify protein quality in chicken meat.

The essential parts of TVB-N are dimethylamine and ammonia (Fallah et al., 2016). TVB-N indicate the proportion of volatile nitrogen-containing compounds in feed ingredients (Ferioli and Caboni, 2010) and suitable to determine the product quality, especially protein feed ingredients (Wojtasik-Kalinowska et al., 2016). Calculation of biogenic ammonia concentration (BAI) was carried out as an index of the freshness of chicken meat due to bacteria (Lázaro et al., 2015; Kozová et al., 2009). Biogenic amine index has proven to be reliable as an indicator in determining the freshness of poultry meat (O'Grady and Kerry, 2008; Silva and Glória, 2002). Ammonia (NH_3) production shows the presence of protein damage in the sample. Damages on protein in chicken meat cause a decrease in ammonia production (Cohen et al., 2007). Protein damage percentage in samples with variations of shelf life is shown in Table 3.

The meat damage is also followed by the formation of sticky mucus

Table 3
Table of protein damage percentage by the MQ 135 sensor.

Sensor	Time (h)	Chicken meat + *E. coli*			Chicken meat		
		NH_3 (ppm)	Level N %	Broken protein %	NH_3 (ppm)	Level N %	Broken protein %
MQ 135	4	4866.6 ± 1.3	3785.1 ± 1.2	2.3 ± 0.1	5511.3 ± 1.5	4286.6 ± 1.6	2.6 ± 0.1
	8	25651.4 ± 2.2	19951.1 ± 1.0	12.4 ± 0.3	10784.6 ± 1.9	8388.0 ± 2.0	5.2 ± 0.1
	12	31914.5 ± 2.8	24822.4 ± 2.3	15.5 ± 0.6	12545.2 ± 2.0	9757.4 ± 1.5	6.1 ± 0.1
	16	35214.5 ± 3.5	27389.1 ± 2.2	17.1 ± 0.6	21920.2 ± 2.0	17049.1 ± 2.5	10.6 ± 0.2
	20	27392.8 ± 2.8	21305.5 ± 3.4	13.3 ± 0.3	15559.2 ± 1.8	12101.6 ± 1.4	7.5 ± 0.2
	24	26705.5 ± 3.3	20771.0 ± 2.6	12.9 ± 0.4	2150.1 ± 1.2	1672.3 ± 1.3	1.1 ± 0.1
MQ 136	4	5310.1 ± 1.0	4130.1 ± 1.0	2.5 ± 0.1	19203.8 ± 2.6	14936.3 ± 1.5	9.3 ± 0.1
	8	6328.9 ± 1.0	4922.5 ± 1.4	3.1 ± 0.1	21125.9 ± 1.5	16431.2 ± 1.6	10.2 ± 0.1
	12	25276.5 ± 2.6	19659.5 ± 2.2	12.2 ± 0.2	24170.1 ± 1.2	18798.9 ± 2.6	11.7 ± 0.1
	16	25917.2 ± 2.3	20157.8 ± 2.2	12.5 ± 0.2	26708.9 ± 2.6	20773.6 ± 2.5	12.9 ± 0.2
	20	22967.1 ± 2.5	17863.2 ± 1.6	11.1 ± 0.2	23040.8 ± 1.6	17920.6 ± 2.5	11.2 ± 0.1
	24	17313.6 ± 2.9	13466.1 ± 1.0	8.4 ± 0.2	21993.1 ± 2.7	17105.7 ± 1.6	10.6 ± 0.1

on the meat surface resulted from the production of dextran, exopolysaccharides or the number of microbial cells growth. On the other hand, the discoloration in chicken meat is caused by the hydrogen sulfide (H_2S) produced during the meat's microbial decomposition. When the protein in chicken meat is damaged, the production of alcohol, ketones, and hydrocarbons (methane and propane) increases significantly over time (Lázaro et al., 2015). In another study, it was reported that color changes in chicken meat with decay occurred because of the production of CO and N (Xiao et al., 2014; Li and Suslick, 2016).

E-nose is a system that detects and recognizes the object based on its odor. The main component of e-nose is the gas sensor with function to measure pollutant gas compounds in the air such as carbon monoxide, hydrocarbons, nitrous oxide, and others. Gas sensors generally detect chemical changes occur in the sensor room, therefore particular sensors are usually placed in a closed room. Heated SnO_2 (tin dioxide) metal oxide crystals at a certain high temperature in air, will cause oxygen to be adsorbed on the crystal surface with a negative charge emitted by the presence of electron donors on the crystal surface which is transferred to the adsorbed oxygen resulting a positively charged space layer. It will produce a surface potential that can inhibit the electrons flow which gives rise to electrical resistance. In the presence of a reducing gas, the density of negatively charged adsorbed oxygen on the semiconductor surface of the sensor is reduced, so that the barrier height at the grain boundary is reduced. The reduced barrier height results in reduced grain sensor resistance in a gaseous environment. The higher concentration value of the sensed gas, the lower its resistance value and inversely the higher the voltage value measured (Triyana et al., 2015).

The voltage pattern of sensor for each sample measured using e-nose shows a typical output pattern that varies based on the sample type and shelf life variation. The longer shelf life of chicken meat does not guarantee gas concentrations continue to increase due to changes in the protein content in chicken meat. Protein damage in the chicken meat started with the fermentation of glucose and glycogen and the breakdown of proteins will form H_2S, indole and amine ammonia compounds. Meat spoilage is also an intensive bacterial decomposition of organic substances which forms odorous gases (Wanniatie et al., 2014). Hence, the odor gas has role as an indicator of decreased freshness of meat.

In this study, we developed a data acquisition system using 6 gas sensors with different specifications for each type. We tested them on chicken meat samples involving treatments of storage period (shelf life) at room temperature, utilizing SVM and SR methods to determine the stored chicken meat quality for consumption. We compared the performance results of this classifier with a chemical analysis for meat protein content. Although we cannot generate a theoretical contribution to the method, we can still provide a theoretical explanation of why the meat is not acceptable to be consumed based on detected gas contamination. At this time, we are still unable to come up with quantitative conclusions about the number of bacteria in the sample or the rate of bacterial growth in chicken meat. Another limitation of this research is, we only observe the voltage response detected by the gas sensors from samples. The sensors reading results have not been compared with analytical methods such as gas chromatography mass spectrometry (GCMS) to determine the composition of gas compounds. However, we believe that in the future this research will be able to provide a quantitative analysis of the bacterial growth rate in chicken meat with more comprehensive data. This quantitative analysis is derived from the relationship between sensor response as a function of gas concentration. More bacteria will produce higher amount of gas, so with the correct transfer function we can calculate the number of bacteria in the sample. Moreover, in the future this research can be conducted by utilizing the deep learning models that will help to improve classical feature extraction techniques, and deep learning can be helpful to implement real time scenario in e-nose.

4. Conclusion

We have demonstrated that the GSA can detect the type of gas in the sample, which is indicated by the appearance of the variance in the sensors output voltage pattern for each sample variation. The data for fresh and contaminated samples were classified with 99.25% and 98.42% precision, respectively by the RF classifier. Furthermore, the SVM classifier correctly identified the fresh and contaminated samples with accuracies of 98.61% and 86.66%, respectively. This finding offers insight into a GSA capability in classifying chicken meat contaminated with *E. coli* using an RF and SVM. Limitation of this study is sole observation of the voltage response generated by the gas sensor to the sample only. The results of the voltage reading produced by the sensor have not been compared with analytical methods such as gas chromatography mass spectrometry (GCMS) in determining the composition of gas compounds.

CRediT authorship contribution statement

Suryani Dyah Astuti: Methodology, Experiments, Validation. **Mohammad H. Tamimi:** Experiments. **Anak A.S. Pradhana:** Methodology, Experiments. **Kartika A. Alamsyah:** Experiments. **Hery Purnobasuki:** Conceptualization, Validation. **Miratul Khasanah:** Methodology, Experiments, Validation. **Yunus Susilo:** Experiments. **Kuwat Triyana:** Conceptualization, Validation, Supervision. **Muhammad Kashif:** Methodology, Experiments. **Ardiyansyah Syahrom:** Conceptualization, Validation, Supervision, All authors participated in the manuscript preparation.

Declaration of competing interest

The authors declare that they have no known competing financial interests or personal relationships that could have appeared to influence the work reported in this paper.

Acknowledgments

We are very grateful to Directorate General Higher Education, Ministry of Research, Technology, and Higher Education and Internal Research Funding of Airlangga University, Surabaya, Indonesia, No. 843/UN3.1.15/PPd/2019 and 372/UN3.14/PT/2020.

References

Abdel-Rahman, E.M., Mutanga, O., Adam, E., Ismail, R., 2014. ISPRS-J. Photogramm. Remote Sens 88, 48–59.
Arshak, K., Moore, E., Lyons, G.M., Harris, J., Clifford, S., 2004. Sens. Rev. 24 (2), 181–198.
Astuti, Suryani D., Puspita, P.S., Putra, A.P., Zaidan, A.H., Fahmi, M.Z., Syahrom, A., Suhariningsih, 2019a. Lasers Med Sci 34 (5), 929–937.
Astuti, Suryani Dyah, Mukhammad, Y., Duli, S.A.J., Putra, A.P., Setiawatie, E.M., Triyana, K., 2019b. J. Med. Signals Sens. 9 (3), 158–164.
Breiman, L., 2001. Random Forests, vol. 45. Kluwer Academic Publishers, pp. 5–32. Machine Learning.
Brudzewski, K., Osowki, S., Markiewicz, T., 2004. Sens. Actuators B Chemical 98 (2–3), 291–298.
Bueno, M., Resconi, V.C., Campo, M.M., Cacho, J., Ferreira, V., Escudero, A., 2013. Food Res. Int. 54 (1), 772–780.
Chang, S., Cohen, T., Ostdiek, B., 2018, 056009 Phys. Rev. 97, 56009, 1 – 6. 97(5).
Chen, C.Y., Lin, W.C., Yang, H.Y., 2020. Respir Res 21 (1), 1–12.
Cohen, N., Ennaji, H., Bouchrif, B., Hassar, M., Karib, H., 2007. J. Appl. Poult. Res. 16 (4), 502–508.
Cortes, C., Vapnik, V., 1995. Mach. Learn. 20, 273–297.
Fallah, F., Ebrahimnezhad, Y., Maheri-Sis, N., Ghasemi-Sadabadi, M., 2016. Arch. Anim. Breed. 59 (2), 191–199.
Fatahi, H., Hossain, M., Sarmadivaleh, M., 2017. J. Nat. Gas Sci. Eng. 37, 409–424.
Ferioli, F., Caboni, M.F., 2010. Eur. Food Res. Technol. 231 (1), 117–126.
Hygreeva, D., Pandey, M.C., 2016. Trends Food Sci. Technol 54, 175–185.
Kodogiannis, V.S., 2017. Food Bioprocess Technol 10 (4), 730–749.
Kozová, M., Kalač, P., Pelikánová, T., 2009. Food Chem 116 (2), 419–425.
Lantz, T.C., Marsh, P., Kokelj, S.V., 2013. Ecosystems 16 (1), 47–59.

Lázaro, C.A., Conte-Júnior, C.A., Canto, A.C., Monteiro, M.L.G., Costa-Lima, B., Cruz, A. G. da, Márs ico, E.T., Franco, R.M., 2015. LWT - Food Sci. Technol. 60 (1), 15–21.
Li, Z., Suslick, K.S., 2016. ACS Sensors 1 (11), 1330–1335.
Men, H., Fu, S., Yang, J., Cheng, M., Shi, Y., Liu, J., 2018. Sensors 18 (1), 1–17.
Mirzaee-Ghaleh, E., Taheri-Garavand, A., Ayari, F., Lozano, J., 2020. Food Anal. Methods. 13 (3), 678–689.
Nitze, I., Barrett, B., Cawkwell, F., 2015. Int. J. Appl. Earth Obs. Geoinf. 34 (1), 136–146.
O'Grady, M.N., Kerry, J.P., 2008. Meat Biotechnol, pp. 425–451.
O'Sullivan, M.G., Byrne, D.V., Jensen, M.T., Andersen, H.J., Vestergaard, J., 2003. Meat Sci 65 (3), 1125–1138.
Oliver, S.P., 2019. Foodborne Pathog. Dis. 16 (7), 439–440.
Pan, L., Zhang, W., Zhu, N., Mao, S., Tu, K., 2014. Food Res. Int. 162–168.
Peris, M., Escuder-Gilabert, L., 2009. Anal. Chim. Acta. 638 (1), 1–15.
Pradhana, A.A.S., Astuti, S.D., Khasanah, M., Ardianti, R.K.D., 2020. AIP. Conf. Proc. 2314.
Premarathne, J.M.K.J.K., Satharasinghe, D.A., Gunasena, A.R.C., Munasinghe, D.M.S., Abeynayake, P., 2017. Food Control 72, 276–282.
Salinas, Y., Ros-Lis, J.V., Vivancos, J.L., Martínez-Máñez, R., Marcos, M.D., Aucejo, S., Herranz, N., Lorente, I., 2012. Analyst 137 (16), 3635–3643.
Silva, C.M.G., Glória, M.B.A., 2002. Food Chem 78 (2), 241–248.
Smolander, M., Hurme, E., Latva-Kala, K., Luoma, T., Alakomi, H.L., Ahvenainen, R., 2002, 3 Innov. Food Sci. Emerg. Technol. 3, 279–288.
Tozlu, B.H., Şimşek, C., Aydemir, O., Karavelioglu, Y., 2021. Biomed Signal Process Control, vol. 64. September 2020.
Triyana, K., Taukhid Subekti, M., Aji, P., Nur Hidayat, S., Rohman, A., 2015. Appl. Mech. Mater. 771, 50–54.
Wanniatie, V., Septinova, D., Kurtini, T., Purwaningsih, N., 2014. J. Ilm. Peternak. Terpadu. 2 (3), 233275.
Wei, Z., Wang, J., 2014. Comput. Electron. Agric. 108, 112–122.
Wijaya, D.R., Sarno, R., Zulaika, E., Sabila, S.I., 2017. Procedia Comput. Sci. 124, 728–735.
Wojnowski, W., Majchrzak, T., Dymerski, T., Gębicki, J., Namieśnik, J., 2017. Meat Sci 131, 119–131.
Wojtasik-Kalinowska, I., Guzek, D., Górska-Horczyczak, E., Głabska, D., Brodowska, M., Sun, D.W., Wierzbicka, A., 2016. *LWT* - Food Sci. Technol. 67, 112–117.
Xiao, K., Gao, G., Shou, L., 2014. Sens. Transducers. 169 (4), 42–48.
Yashoda, K.P., Sachindra, N.M., Sakhare, P.Z., Narasimha Rao, D., 2001. J. Food Qual. 24 (3), 249–259.